Quantum dynamics of adsorbed normal- and para-H_2, HD, and D_2 in the microporous framework MOF-74 analyzed using infrared spectroscopy

S. A. FitzGerald, J. Hopkins, B. Burkholder, and M. Friedman
Department of Physics and Astronomy, Oberlin College, Oberlin, Ohio 44074, USA

J. L. C. Rowsell
Department of Chemistry and Biochemistry, Oberlin College, Oberlin, Ohio 44074, USA

(Received 29 August 2009; revised manuscript received 23 December 2009; published 29 March 2010)

Low-temperature diffuse reflectance infrared spectroscopy is used to measure the quantum dynamics of molecular hydrogen and its isotopologues adsorbed in the microporous material MOF-74. At least two distinct adsorption sites are revealed by increasing the concentration of H_2 within the material and monitoring the successive appearance of absorption bands with decreasing bathochromic shifts (or "redshifts") from the unperturbed (gas-phase) vibrational frequencies. Under conditions wherein both the primary and neighboring secondary sites are occupied, additional frequency shifts are observed that confirm the interactions among the adsorbed molecules are non-negligible. *Ortho* to *para* conversion of the adsorbed *normal*-H_2 is observed to occur within minutes and this process is accelerated when both primary and secondary sites are occupied. Translational sidebands are also observed, providing an estimation of 124 cm^{-1} for the frequency of the center-of-mass motion of H_2 at the primary adsorption site. The frequency shifts of the absorption bands of HD and D_2 diverge from the predictions of a simple isotope effect, emphasizing the importance of the zero-point energy contribution.

DOI: 10.1103/PhysRevB.81.104305 PACS number(s): 78.30.−j, 82.75.−z

I. INTRODUCTION

The inability to store hydrogen in adequately large densities under ambient conditions remains a daunting obstacle to the proliferation of fuel cell powered vehicles. There remains no sorbent material yet identified that can gainfully circumvent the hundreds of atmospheres of pressure or hundreds of degrees of cooling that are employed in traditional hydrogen containment systems. Such a compound should not only condense the supercritical, flammable gas under ambient conditions to a density comparable to that of solid H_2, it must also release the gas on demand while contributing minimal mass to the system.

Physisorbents, materials that adsorb intact H_2 molecules within the pores of their structures, have inherently superior uptake and release kinetics and would be favored for mobile fueling if a representative exhibited both (1) a very large specific micropore volume and (2) an adsorption enthalpy that remains sufficiently large (in magnitude) as hydrogen is loaded. A few materials satisfy the first criterion[1–7] but their impressive adsorption capacities are only realized below approximately 100 K. This is because their adsorption enthalpies are substantially smaller than the calculated target of −15 kJ/mol,[8] in some cases precipitously falling in magnitude after preferential adsorption sites are filled. Consequently, interest is now focused on identifying chemical moieties that are strongly attractive to H_2 so that these may be incorporated with greater surface density in future materials.

Available techniques for quantifying the strength of H_2-to-adsorbent interactions are limited in the level of detail they provide. The most commonly employed method is the isosteric analysis of H_2 adsorption isotherms measured using liquid nitrogen and liquid argon as cryogens.[3–7] The analysis yields the range of adsorption enthalpy exhibited by a material as it is loaded with H_2 but does not provide site-specific information. Similarly, temperature-programmed desorption[9,10] and adsorption calorimetry[2,11] results describe the distribution of enthalpies afforded by an array of adsorption sites but alternate techniques are required to map out these chemical landscapes. The structural details of adsorption sites in crystalline adsorbents can be gleaned from neutron diffraction experiments,[3,6,12–17] however, the relative binding energies of the sites must be inferred from their sequential population as adsorption progresses.

Spectroscopic analyses can, in principle, discriminate H_2 molecules based on their adsorption sites and directly provide information about the energetics of their local interactions. In one method, thermal neutrons are inelastically scattered by adsorbed H_2, yielding an energy-loss spectrum that describes the hindered rotational transitions of these molecules. The rotational energy levels are strongly dependent on the chemical environment of the adsorption site and are related to the adsorption enthalpy in a complex manner that has yet to be fully understood.[5,9,18–21] Infrared (IR) spectroscopy provides a complementary technique, wherein absorptions due to H_2 (ro)vibrational transitions are weakly activated by interactions with surface atoms.[11,22–30] The spectral features also convey information about the symmetries and interaction potentials of the adsorption sites. Importantly, IR spectroscopy boasts rapid data collection; consequently, variable-temperature experiments are tractable, which can provide site-specific enthalpies and entropies of adsorption using a van't Hoff-derived analysis.[25,26,28,30,31] Finally, Raman spectroscopy has been employed to a lesser extent, with very small shifts in the vibrational resonances of H_2 being observed.[32–34] Correlations with adsorption enthalpies have not yet been established.

Recently, we examined hydrogen adsorption by the model microporous coordination framework $Zn_4O(bdc)_3$ (bdc

=benzene-1,4-dicarboxylate), known as MOF-5 and IRMOF-1, using diffuse reflectance IR spectroscopy at low temperatures.[29] The results corroborate the site-filling model developed in previous x-ray diffraction,[35] neutron diffraction,[12,13] and inelastic neutron scattering reports;[19] specifically, that small, inert molecules such as H_2 preferentially adsorb to faces of the framework's inorganic clusters, followed by adsorption on the less attractive organic moieties. In addition, the observed vibrational redshifts were used to estimate site-specific adsorption enthalpies, yielding values comparable to those of theoretical predictions and site-averaged enthalpies measured by isosteric analyses.

Our next material of interest is the *catena*-(μ_8-2,5-dioxidobenzene-1,4-dicarboxylato)dizinc(II) compound referred to in the literature as MOF-74 (Ref. 36) and CPO-27-Zn.[37] Like MOF-5, the material has a simple, high-symmetry, periodic structure that defines a large micropore volume. The pore array consists of a hexagonal "honeycomb" of parallel channels that are 1.1 nm in diameter (after accounting for the van der Waals radii of the framework atoms). The pore walls are lined with Zn^{2+} cations in square pyramidal coordination, exposing the Zn—O dipoles to a greater extent than in MOF-5. These structural features result in a substantially larger H_2 adsorption enthalpy in MOF-74, as evinced by isosteric analysis.[38] Interestingly, the derived heat of adsorption (defined as the negative of the adsorption enthalpy) rises by a small amount initially with loading, suggesting the action of non-negligible $H_2 \cdots H_2$ attractions. These are typically ignored in theoretical models and simulations of hydrogen adsorption; consequently, experimental evidence of their importance is highly valuable. This has recently been supplied by a combined neutron diffraction and inelastic neutron scattering study of hydrogen in MOF-74, wherein very short (2.9 Å) nearest-neighbor distances between the adsorbed molecules were refined.[39] To complement these results, we have independently synthesized the material and examined its affinity for molecular hydrogen and its isotopologues using diffuse reflectance IR spectroscopy.

Mid-IR spectroscopy probes excitations in which H_2 undergoes a vibrational transition. This may also be accompanied by a change in the rotational quantum number J; however, quantum statistics constrain H_2 molecules with total nuclear spin $I=1$ (*ortho*-hydrogen, *o*-H_2) to have an odd J quantum number while those with $I=0$ (*para*-hydrogen, *p*-H_2) have even J.[40] Consequently, transitions are limited to $\Delta J=0$ or ± 2. If $\Delta J=0$ the transitions are purely vibrational and denoted as $Q(J)$ transitions. If $\Delta J=+2$, the H_2 also undergoes an excitation of its rotational state, which is referred to as a rovibrational transition and labeled $S(J)$. There are four possible transitions at low temperature: $Q(0)$ and $Q(1)$, which differ by only 6 cm^{-1}, along with $S(0)$ and $S(1)$. As discussed at greater length in our previous paper,[29] an isolated H_2 molecule is IR inactive but interactions with neighboring atoms activate these transitions and often cause band splitting and shifting of their frequencies. These perturbations provide information about the symmetry and interaction energy specific to an adsorption site. The results presented here reveal at least two distinct adsorption sites in MOF-74. Sequential site filling is tracked by comparing band intensities at several H_2 concentrations; when neighboring adsorption sites become populated, the shifting of bands in the Q, $S(0)$, and $S(1)$ regions are observed that provide further evidence of $H_2 \cdots H_2$ interactions. Additionally, the importance of accounting for the adsorbate molecules' zero-point energies (ZPEs) is confirmed by comparing spectra of *para*-H_2, HD, and D_2, which show a systematic deviation from classical predictions.

II. EXPERIMENTAL SECTION

Samples of crystalline, high-purity $Zn_2(C_8H_2O_6)$ (MOF-74) were prepared using an establishing solvothermal synthesis, employing *N*,*N*-dimethylformamide and water for crystal growth and methanol as the activation solvent.[38] Removal of these molecules from the pores of the framework was achieved by heating the material to 250 °C under a flow of dry nitrogen for 8 h. A comparable synthetic procedure was exercised by Liu *et al.* for their analyses, wherein the material's hydrogen adsorption properties were confirmed.[39]

The compositional purity of the sample used for this paper was established by thermogravimetric analysis (TGA), with instrumental details and data provided in the supplementary information.[41] Between room temperature and 200 °C, the outgassed material loses $<2\%$ mass, this small amount being attributable to atmospheric moisture quickly adsorbed during transfer of the sample from the inert atmosphere in which it was stored. Under a flow of dry air, the material undergoes a two-step combustion (onset temperatures, $T_{onset}=273$ and 338 °C) to yield ZnO, liberating 50.8% of the mass measured at 200 °C. This is in agreement with the expected 50.1% mass loss for this process. When dry nitrogen is used as the purge gas, significant mass loss is forestalled until $T_{onset}=392$ °C. TGA of the methanol-exchanged material revealed the same decomposition processes, following loss of surface- and channel-bound solvent amounting to 28% of the initial mass. The phase purity of the crystalline fraction of the outgassed sample was established by powder x-ray diffraction (PXRD), with instrumental details and data provided in the supplementary information.[41] The measured pattern is in agreement with that calculated from the refined structure of the empty framework reported by Dietzel *et al.*[37] This variable-temperature PXRD study identified five phases of differing degrees of hydration that are easily distinguishable by their PXRD patterns.[42] No extraneous reflections were found in our measured pattern to indicate the presence of crystalline impurities; furthermore, the reflections are sharp, indicating the framework has maintained order following outgassing.

Spectroscopic analyses of molecular hydrogen and its isotopologues adsorbed within the channels of MOF-74 were performed using a custom-built diffuse reflectance system. The sample chamber allows both the temperature and atmospheric environment of the material to be controlled, as detailed in a recent publication.[43] IR spectra were acquired using a Bomem DA3 Michelson interferometer equipped with a quartz-halogen source, CaF_2 beamsplitter, and a liquid-nitrogen-cooled mercury-cadmium-telluride detector. Samples ($\sim$10 mg) were transferred under inert atmosphere

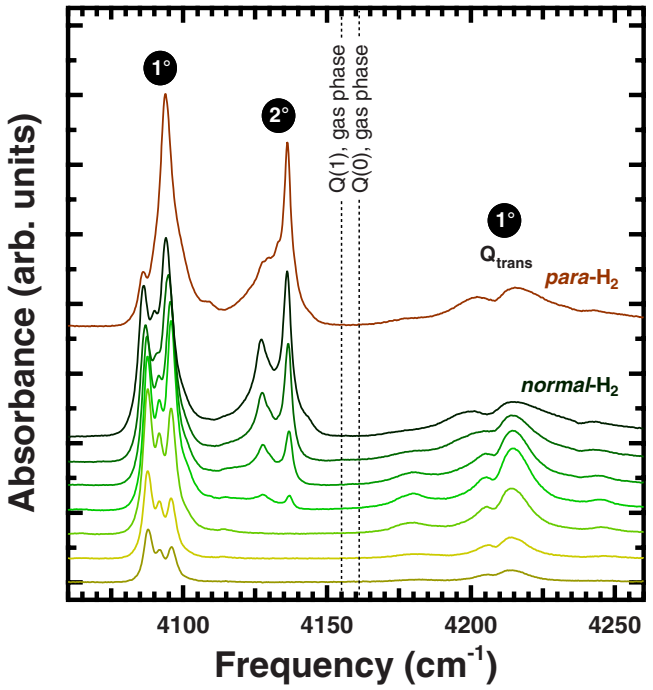

FIG. 1. (Color online) Diffuse reflectance spectra of adsorbed H_2 in MOF-74 with loadings of 0.15, 0.25, 0.5, 0.85, 1.3, 1.6, and 2.0 H_2 per Zn. Data were collected at 40 K; spectra are vertically offset for clarity. Band assignments are labeled according to their adsorption site, primary (1°) and secondary (2°) with Q_{trans} denoting a translational sideband. The spectrum of 1.8 *para*-H_2 per Zn is shown as the uppermost trace (brown).

to a cup affixed to a copper slab providing thermal contact to a cold-finger cryostat (Janis ST-300T). Prior to introduction of the analyte gas, the samples were evacuated for several hours at room temperature. Known quantities of research grade (99.9999% purity) H_2, HD, or D_2 were dispensed from a calibrated gas manifold by monitoring the change in pressure. *Para*-enriched H_2 was prepared by the procedure of Andrews and Wang.[44]

III. RESULTS AND DISCUSSION

A. Vibrational spectroscopy

There are three spectral regions of interest where H_2 vibrational and rovibrational transitions are expected: the Q region around 4160 cm^{-1}, $S(0)$ region near 4500 cm^{-1}, and the $S(1)$ region proximate to 4700 cm^{-1}. Our analysis of H_2 in MOF-74 has uncovered features in each of these regions, as described sequentially below.

Spectra containing bands assigned to the purely vibrational Q transitions of adsorbed H_2 in MOF-74 are presented in Fig. 1. As observed in previous studies,[22,29,30] features with large redshifts appear at the lowest concentrations and are assigned to H_2 adsorbed on preferential sites, i.e., those with the largest site-specific adsorption enthalpy. In MOF-74, three bands are found at 4088, 4092, and 4096 cm^{-1}. As the material is loaded further, all three bands grow in intensity until the stoichiometry approaches 1 H_2 per Zn cation, after which there is a small redistribution of intensity from the 4088 and 4092 cm^{-1} bands to the 4096 cm^{-1} band. We attribute this change in intensity to *ortho* to *para* conversion and provide further evidence for this assessment in Sec. III D. The most notable point here is that above a concentration of 1 H_2 per Zn there is no additional gain in intensity by these bands, indicating that the crystallographic adsorption site with which they are associated is saturated. This supports the findings of Liu *et al.*, who refined crystallographic models of localized D_2 molecules in this framework as a function of loading.[39] At 4 K, they found complete occupation of one adsorption site at a concentration of 1 D_2 per Zn while other possible sites remained vacant. The position of this site is directly above the base of the square pyramidal ZnO_5 coordination environment, where the Zn—O dipoles are most exposed within the channels. This is the most reasonable site for preferred adsorption because it is the position of maximal electrostatic interaction. Crystallographically, it can accommodate one adsorbate molecule per Zn; these consistencies with our observations lead us to assign the three bands at 4088, 4092, and 4096 cm^{-1} to H_2 adsorbing on this primary site.

A second series of bands appears in the frequency range 4128–4137 cm^{-1} as the material is loaded with more hydrogen. As shown in Fig. 1, they first appear at a loading of 0.85 H_2 per Zn, close to where the primary site saturates, and continue to increase in intensity with the addition of more H_2. That these bands also exhibit a smaller redshift from the gas-phase frequencies attests to their origin as that of H_2 on secondary adsorption sites. With reference to the neutron diffraction work of Ref. 39, one is positioned above an edge of the ZnO_5 square pyramid, with the closest oxygen <3.4 Å away, and another is above an edge of the benzenoid ring, with two carbons <3.1 Å away.[45] The refined models suggest that the former site is occupied first among this pair, and so we tentatively assign the cluster of bands surrounding 4128 and 4137 cm^{-1} to the ZnO_5-edge site, recognizing that overlap of multiple bands in this region could indicate either multiple site contribution, splitting of bands due to symmetry reduction or both.

The occupation of the secondary sites also has a significant effect on the bands arising from molecules adsorbed at the primary site. Upon loading the material with 2.0 H_2 per Zn, the three bands associated with the primary site are redshifted an additional 2 cm^{-1}. This points to positive reinforcement of this site's adsorption enthalpy by adsorbate-adsorbate interactions. According to the crystallographic work described in Ref. 39, the intersite distance between neighboring symmetry equivalents of the primary site is 5.3 Å, thus they are quite isolated. By comparison, the secondary sites are <3.2 Å away (the distances changing somewhat with loading), closer than the nearest neighbors in solid H_2 (3.8 Å).[46] Given that the 12 nearest neighbors in the solid phase produce a 6 cm^{-1} redshift,[46,47] it is reasonable that a smaller number of closer interactions could produce the redshift we observe from this adsorbed phase.

To assist in delineating the rotational states of the transitions, we studied the adsorption of *para*-enriched H_2. As noted in Table I and indicated in Fig. 1, the $Q(0)$ and $Q(1)$ transitions of gaseous H_2 are separated by 6 cm^{-1}. External interactions can alter this separation and also cause a split-

TABLE I. Frequencies (cm^{-1}) of the strongest H_2 in MOF-74 $Q(0)$, $Q(1)$, $S(0)$, and $S(1)$ transitions classified by adsorption site.

Site	$Q(0)$	$Q(1)$	$S(0)$	$S(1)$
Gas	4161.2	4155.3	4497.8	4712.9
Primary	4096.0	4087.9	4364.3	4586.8
		4092.0		4609.7
	4219[a]	4209[a]		
Secondary	4136.9	4128.0	4450.0	4689.3
			4484.9	

[a]Refers to center-of-mass translational bands.

ting of the $Q(1)$ transition. Band overlap due to the latter effect is avoided by analyzing p-H_2, which only exhibits $Q(0)$ transitions. Shown at the top of Fig. 1 is the spectrum of MOF-74 loaded with 1.8 p-H_2 per Zn. Upon comparison with the spectrum of the same amount of *normal*-H_2 in the framework, the $Q(0)$ transitions are easily identified as the highest frequency band in each grouping, i.e., 4094 cm^{-1} (shifted from 4096 cm^{-1} at small loadings) and 4136 cm^{-1} (shifted from 4137 cm^{-1}). Minor remnants of the $Q(1)$ bands 6 cm^{-1} lower in frequency from these two bands are due to incomplete *para* enrichment of the H_2 and/or *para* to *ortho* backconversion to thermal equilibration at 40 K, which we describe in Sec. III D. The shoulders at 4130 and 4134 cm^{-1} appear to be more $Q(0)$ than $Q(1)$-like in behavior, perhaps arising from H_2 at the other sites elucidated by neutron diffraction.[39]

B. Center-of-mass translational mode

In addition to the sharp, redshifted bands in the Q region, there are also significantly broader features that appear at higher frequencies than the gas-phase values. The strongest of these, centered at 4215 cm^{-1}, has a concentration dependence associated with the primary site. It has been shown for other systems that these broader bands arise from transitions in which the adsorbed H_2 also increases its center-of-mass translational motion (akin to rattling back and forth within the adsorption site) by one quantum.[27,29,48] Weaker features observed at 4180 and 4245 cm^{-1} can be ascribed to translational excitations with a different direction of motion within the primary site. In each case, the bands have both *ortho* and *para* components (see Sec. III D), with the *para* component at expectedly higher frequency.

Taking the $Q(0)$ band at 4096 cm^{-1} as the pure vibrational frequency that corresponds to the *para* component of the 4220 cm^{-1} band, its translational frequency can be determined as 123 cm^{-1}. This is in good agreement with the recent prediction of 122 cm^{-1} by Kong *et al.* using van der Waals density-functional calculations.[49] As noted, inelastic neutron scattering experiments, such as recently performed by Liu *et al.*,[39] are insensitive to these transitions since the low-temperature translational peak intensity is controlled by the relatively weak coherent cross section. The translational frequency of 123 cm^{-1} is larger than that observed for other microporous coordination frameworks,[27,29] and comparable

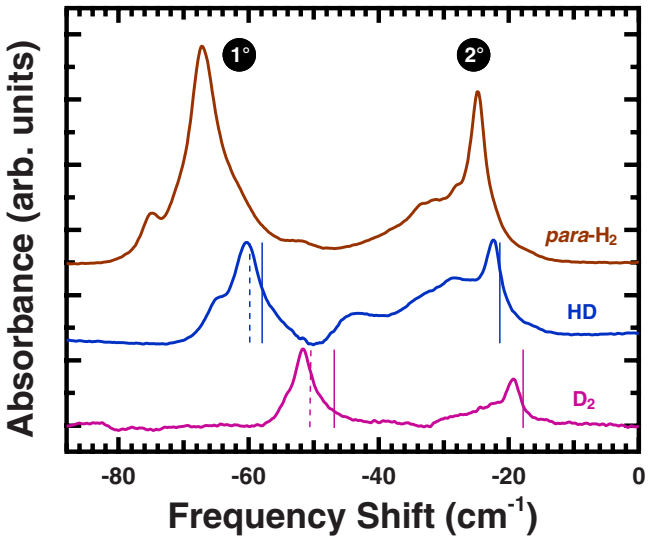

FIG. 2. (Color online) Q-region spectra of isotopologues adsorbed in MOF-74 (1.8 *para*-H_2 per Zn, 2.0 HD per Zn, and 2.1 D_2 per Zn) at 40 K. Each spectrum has been frequency shifted by the corresponding $Q(0)$ gas-phase value and the traces are vertically offset for clarity. Bands assigned to molecules adsorbed on the primary (1°) and secondary (2°) sites follow the trend predicted by simple reduced mass scaling ($\frac{1}{\sqrt{\mu}}$, solid lines). The predicted frequencies are in better agreement when zero-point energy effects are included (dashed lines).

to H_2 confined in solid argon[50] and the interstices of the C_{60} lattice.[48] We note the general trend that systems with larger binding energies tend to yield higher H_2 translational frequencies. Approximating the center-of-mass translation as that of a three-dimensional simple harmonic oscillator yields a ZPE of 2.1 kJ/mol, in good agreement with the theoretical prediction of 2.0 kJ/mol with a 5–10 % level of anharmonicity.[49] This is a significant fraction of the adsorption enthalpy derived for the preferred sites by isosteric analysis (8–9 kJ/mol),[38,39] indicating that quantum-mechanical effects are indeed critical to any detailed theoretical modeling.

A final observation from this region is the broadening of the translational bands as the largest H_2 concentration is approached (see Fig. 1). This is coincident with the redshifting of the primary site Q bands that occurs upon population of secondary adsorption sites, and provides further evidence for $H_2 \cdots H_2$ interactions.

C. Vibrational spectroscopy of hydrogen isotopologues

To further demonstrate the importance of quantum considerations when examining adsorbed molecular hydrogen, we studied the isotopologues HD and D_2. Figure 2 compares the spectra acquired after loading comparable molar amounts of these gases and p-H_2 in MOF-74; both primary and secondary sites are populated in each case. The spectra have been offset in frequency by the corresponding $Q(0)$ gas phase values to provide a common scale. The x axis measures the frequency shift induced by adsorption on the framework sites. Prominent $Q(0)$ bands are observed for p-H_2, with

weak $Q(1)$ bands present due to incomplete enrichment or backconversion (*para* to *ortho*, evidence of which is provided below). *Normal*-D_2 was employed; the apparent absence of a $Q(1)$ in this spectrum is due to the reduced $Q(0)-Q(1)$ difference (2 cm^{-1} for the gas phase), which hampers resolution of the individual bands.

An isotope effect on the band intensities is observed with $H_2 > HD > D_2$ (see Fig. 2). This is consistent with the general IR rule that intensity is proportional to $\nu|\langle i|D|f\rangle|^2$ (Ref. 40), where ν is the frequency of the absorbed photon and $|\langle i|D|f\rangle|$, the induced dipole moment matrix element linking the initial to final state, is equivalent to the intrinsic polarizability element used in determining Raman intensities.[51]

The primary site vibrational redshifts are 66.1 cm^{-1}, 59.6 cm^{-1}, and 51.6 cm^{-1} for *p*-H_2, HD, and D_2, respectively. For the secondary site, the respective values are 24.3, 22.0, and 19.4 cm^{-1}. This trend is approximated by the simple scaling model in which the frequency shift is proportional to the inverse of the square root of the reduced mass (marked by solid lines in Fig. 2).[52] The origin of this shift is the change in binding energy, E_b, between the vibrational ground and excited states. Anharmonicity in the H_2 vibrational motion results in an increased H—H bond length, which alters its interaction with the framework.[50] The interactions are stronger for vibrationally excited H_2, yielding a typically positive correlation between E_b and the redshift of the mode.[53] This is dominated by changes in the polarizability and quadrupole moment of the molecule, which have been shown to scale quadratically with the H—H internuclear separation.[54] It is well known that for a simple harmonic oscillator,

$$\langle x^2\rangle = \left(n+\frac{1}{2}\right)\frac{\hbar}{\mu\omega} = \left(n+\frac{1}{2}\right)\frac{\hbar}{k}\frac{1}{\sqrt{\mu}}, \tag{1}$$

where n is the vibrational quantum number, ω the vibrational frequency, μ the reduced mass, and k, the molecular spring constant. Since the value of k is essentially the same for H_2, HD, and D_2, Eq. (1) shows that the change in $\langle x^2\rangle$ scales as $1/\sqrt{\mu}$ and hence to a first approximation both the change in E_b and the vibrational redshift will also scale as $1/\sqrt{\mu}$.

It is clear from Fig. 2 that this simple model is insufficient to accurately relate the redshifts of the isotopologue bands. Including the known differences in the deviations from simple harmonic-oscillator behavior among H_2, HD, and D_2 produces very minor (<1%) corrections to the $1/\sqrt{\mu}$ predictions of Eq. (1). A more important consideration is the ZPE of the center-of-mass translational motion of the adsorbate molecules. For the primary site, we estimate the ZPE by approximating the motion as that of a three-dimensional simple harmonic oscillator. This yields values of 2.1 kJ/mol, 1.8 kJ/mol, and 1.5 kJ/mol for H_2, HD, and D_2, respectively. A more rigorous treatment would include anharmonic contributions which have been estimated by Kong *et al.* to be on the order of 5–10 %,[49] leading to corrections that are inconsequential relative to the uncertainty in the estimates made below. The more massive D_2, having a smaller ZPE, resides deeper in the potential well formed by the interactions with the framework atoms, thereby experiencing a greater binding energy and a correspondingly larger vibrational redshift. We can quantify this effect by noting the general relationship that the redshift is on the order of 10% of the binding energy.[29] This provides an estimate of 8.2 kJ/mol for the primary site H_2 adsorption enthalpy, in agreement with reported isosteric values at low loading,[38,39] and correspondingly larger values for HD and D_2 (8.5 kJ/mol and 8.8 kJ/mol, respectively). Using the same correlation, predictions for the redshifts of the heavier isotopologues can be made that are in improved agreement with the experimental values, as shown in Fig. 2. The redshifts of the secondary bands exhibit a similar trend; however, the corresponding translational bands were not observed to provide data for the ZPE corrections.

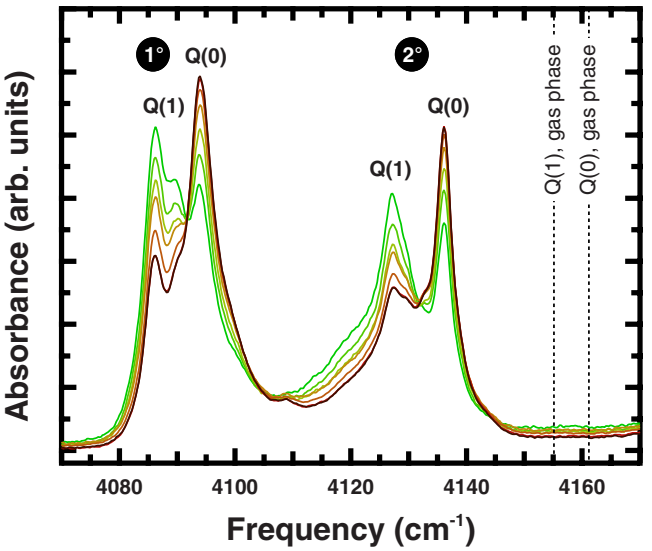

FIG. 3. (Color online) Evolution of the Q-region bands assigned to the primary (1°) and secondary site (2°) with accelerated *ortho* to *para* conversion. Traces proceed from green to brown, collected at t=55, 95, 135, 175, 280, 600, and 2700 s after loading 1.8 H_2 per Zn at 40 K. The spectrum collected after 2700 s (dark brown) shows almost no change from that at 600 s.

D. *Ortho* to *para* conversion

Another quantum dynamical behavior that aids the assignment of these IR spectral features is *ortho* to *para* conversion. As demonstrated in our recent study of MOF-5,[29] the loss of intensity from bands over time indicates that they are assignable to *o*-H_2 and must therefore be $Q(1)$ or $S(1)$ transitions; the converse being true for *p*-H_2. In solid or liquid hydrogen, the time constant for conversion is on the order of hours while the gas phase can be maintained far from thermal equilibrium for many days.[55] Pertinent to undertaking spectroscopic experiments is the recognition that an arbitrary H_2 spectrum obtained at 40 K could arise from an *ortho*:*para* ratio anywhere between the room-temperature value of 3:1 and the equilibrium value of roughly 1:8. In most adsorbents the ratio remains close to 3:1 for several hours, however, we observed extremely fast conversion in MOF-74, on the order of minutes.

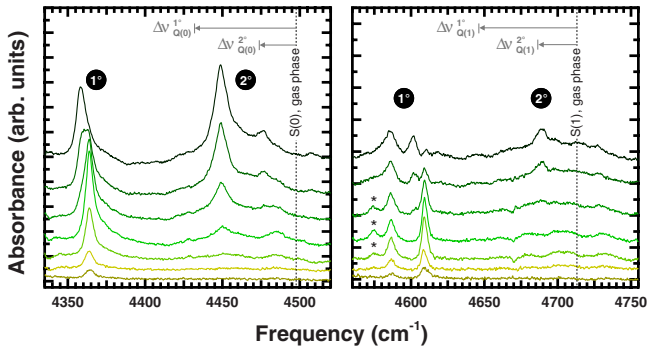

FIG. 4. (Color online) $S(0)$ transitions (left) and $S(1)$ transitions (right) in the diffuse reflectance spectra of adsorbed H_2 in MOF-74 with loadings of 0.15, 0.25, 0.50, 0.85, 1.3, 1.6, and 2.0 molecules per Zn. Data were collected at 40 K, spectra are vertically offset for clarity. Bands are labeled according to their assigned adsorption site, primary (1°), and secondary (2°). The redshifts of the corresponding Q transitions are indicated with arrows.

The Q-region spectra shown in Fig. 3 illustrate the dramatic transfer in intensity for both the primary and secondary site bands during the few minutes immediately after loading. The loss of intensity from the primary site bands at 4088 and 4092 cm^{-1} and secondary site band at 4128 cm^{-1} confirms these as $Q(1)$ bands while the concurrent increases at 4096 and 4137 cm^{-1} indicate $Q(0)$ bands. Similar behavior for the translational bands centered around 4215 cm^{-1} (not shown) confirms that they arise from both *ortho* and *para* species. The rovibrational S bands, discussed in detail in the next section, also demonstrate the expected changes in intensity with time.

Unlike the exposed Cu^{2+} cations in the framework HKUST-1,[30] there are no obvious paramagnetic centers in MOF-74 that we can point to as performing spin catalysis. While we have observed rapid spin conversion on multiple samples from different sources it is still possible that the effect may be due to a common magnetic impurity. Regardless, *ortho* to *para* conversion provides a useful method for distinguishing between $Q(0)$ and $Q(1)$ excitations.

E. Rovibrational bands

An important advantage of the diffuse reflectance technique is its ability to enhance weak absorption features relative to strong ones.[24] Relevant to these studies is the opportunity to observe additional vibrational transitions involving concomitant rotational excitation. While the purely vibrational Q transitions arise from both the overlap and quadrupole mechanisms, the S transitions stem almost entirely from the latter process.[47] Consequently, the S bands are weak for H_2 and essentially unobservable for HD and D_2, for which there are also strong framework absorptions in the corresponding spectral regions.

Multiple rovibrational bands are observed in both $S(0)$ and $S(1)$ spectral regions for H_2 adsorbed in MOF-74. As shown in Fig. 4(a), there are three main $S(0)$ features in the 4350–4500 cm^{-1} range, comprising a primary site band at 4364 cm^{-1} that appears at the lowest loadings and a pair of secondary bands at 4450 and 4485 cm^{-1} that becomes evident at 0.85 H_2 per Zn, in concert with the secondary Q bands described earlier. Another similarity to the Q region is the notable frequency shift in the principle $S(0)$ band upon filling of the secondary sites. In this case, the loading dependence suggests a discrete, shifted band increases in intensity while the original band decreases.

The primary $S(0)$ band has a large initial redshift of 133 cm^{-1} relative to the gas phase, more than twice the redshift of the primary $Q(0)$ band. At the simplest level, the $S(0)$ frequency shift can be described in terms of a vibrational contribution comparable to that of the $Q(0)$, 65 cm^{-1}, plus an additional amount arising from the splitting and shifting of the $J=2$ rotational level compared to $J=0$. This large shift is indicative of a highly anisotropic site potential with a strong rotational-translational coupling, as initially suggested by INS spectra of the $J=0$ to $J=1$ transition.[39] The absence of other $S(0)$ bands associated with the primary site is surprising since, in general, one would expect to observe multiple transitions to the nondegenerate $J=2$ sublevels. Possible explanations are that Δm selection rules have diminished their intensities and/or lifetime broadening of the excited $J=2$ sublevels occurs to such an extent that the bands are undetectable.

The redshifts of the secondary $S(0)$ bands (47.8 and 12.9 cm^{-1}) are comparable to those of the secondary $Q(0)$ bands. The appearance of a band at slightly higher and lower frequencies is consistent with a symmetric splitting of the $J=2$ sublevels.

Rapid *ortho* to *para* conversion presents a challenge to the observation of $S(1)$ bands. Each feature corresponds to a vibrational transition simultaneous with a rotational transition from $J=1$ to $J=3$; they therefore lose intensity as o-H_2 is depleted during thermal equilibration at low temperature. Our findings in this spectral region are displayed in Fig. 4(b). There are two primary site bands at 4587 and 4610 cm^{-1} that appear at small H_2 loadings, accompanied by an artifact of the background subtraction at 4578 cm^{-1}, where there is a strong framework absorption band. At the largest loadings, a dramatic shift in the primary $S(1)$ band is observed—as remarked upon for the primary Q and $S(0)$ bands—along with the appearance of a secondary band at 4689 cm^{-1}. In this region, it is even more apparent that populating a secondary site leads to the introduction of a new primary band that grows at the expense of the original. In contrast, the other primary band at 4610 cm^{-1} broadens but does not display a frequency shift.

F. Hindered rotor model

Recently, Kong *et al.*[49] used a standard hindered rotor model to deduce the rotational level splitting of H_2 at the primary site of MOF-74. The orientational potential is expanded in terms of spherical harmonics with the Y_0^0 coefficient dominating the overall binding energy and the Y_2^m coefficients determining the actual level splitting. The coefficients indicate a maximum rotational barrier of 28 meV

and produce reasonable agreement with reported inelastic neutron scattering data,[39] although the predicted transition energies are roughly 20% greater. We now extend this model to the mid-IR by assuming that the interaction potential for H_2 in its vibrationally excited state is 10% greater than in its ground state[53] and that all rovibrational transitions have the same pure vibrational frequency of 4096 cm^{-1}. This leads to predictions that at 40 K there should be $Q(1)$ peaks at 4088 and 4090 cm^{-1} in comparison to the experimental values of 4087 and 4092 cm^{-1}. Agreement with the $S(0)$ transitions is less satisfactory with the model predicting four possible transitions ranging from 4398 to 4510 cm^{-1} while experiment shows a single band at 4364 cm^{-1}. $S(1)$ bands are predicted to occur from the two thermally populated $J=1$ sublevels to the five $J=3$ sublevels. This leads to a set of five transitions ranging in frequency from 4644 to 4755 cm^{-1} and a second set of five ranging from 4621 to 4733 cm^{-1}. In comparison, experiment shows two $S(1)$ bands at 4587 and 4610 cm^{-1}.

As stated above, absence of additional experimental S bands is most likely due to the combination of Δm selection rules and lifetime broadening. The observed S bands are quite weak and any significant reduction in intensity would render them undetectable. Deduction of the Δm selection rules requires a vector sum over the polarizability of the host ions which has proved challenging even for the simple C_{60} system[56] and is presently intractable for a complex system such as MOF-74. However, the model would suggest that the observed bands correspond to transitions to the lowest possible J sublevel, with the predicted $S(0)$ transitions at 4398 cm^{-1} (in comparison to the experimental 4364 cm^{-1}) and $S(1)$ transitions predicted at 4621 and 4644 cm^{-1} (in comparison to the experimental 4587 and 4610 cm^{-1}).

In each case, the theoretical values predict a rotational transition roughly 10% higher than experiment. This is consistent with the level of agreement found with neutron data.[49] Mulder *et al.* observed similar behavior for H_2 in MOF-5 and used an apparent rotational constant reduced by as much as 30% from free H_2 to produce agreement with experiment.[20] We believe that a more physically reasonable explanation is the need for inclusion of rotational-translational coupling which will be quite strong for systems in which the translational and rotational transitions are similar in frequency.

G. Comparison of MOF-5 and MOF-74

We conclude this paper by comparing results from the two high-symmetry microporous zinc carboxylate frameworks we have examined thus far. As noted in Sec. I, MOF-5 and MOF-74 have considerably different surface features and pore dimensions; this dissemblance is clearly manifested in the IR absorption features of H_2 adsorbed within their open frameworks. Figure 5 compares spectra for which both the primary and secondary sites of each material are populated. Several differences in the spectra exist: (i) MOF-74 exhibits larger vibrational redshifts, (ii) MOF-5 has sharper bands, requiring a higher instrumental resolution with concomitantly larger background noise, (iii) MOF-5 has S-band intensities that are comparable to those of the Q bands, and (iv) MOF-5 shows a distinct orientational transition. The last two

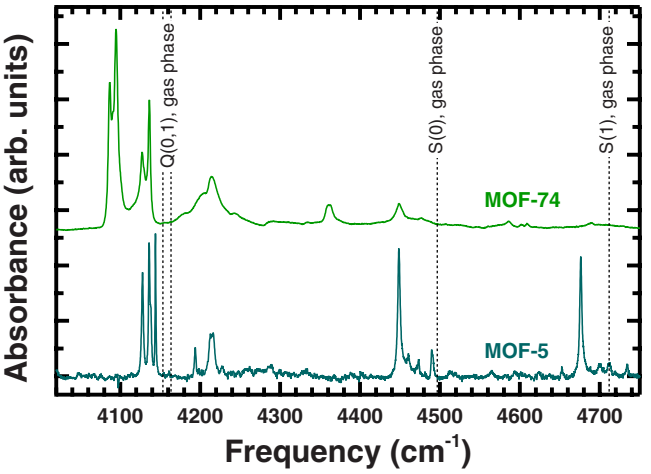

FIG. 5. (Color online) Comparison of the diffuse reflectance IR spectra of *normal*-H_2 adsorbed in MOF-74 (upper trace) and MOF-5 (lower trace). MOF-74 was loaded with 1.6 molecules per Zn and examined at 40 K using a resolution of 0.5 cm^{-1} while MOF-5 was loaded with 1.5 molecules per Zn and examined at 30 K using a resolution of 0.25 cm^{-1}. Spectra have been vertically offset for clarity. MOF-5 data were previously reported in Ref. 29.

characteristics are consistent with a strong quadrupole mechanism contributing to the IR activity since this gives rise to a change in the m quantum number. S bands with comparable intensity to the Q have been reported for both H_2 in the interstices of solid C_{60} (Ref. 48) and the endohedral species $H_2@C_{60}$.[57]

Shared between both materials is the initial appearance of Q and S bands that are strongly redshifted, followed by additional bands with smaller redshifts that become evident at larger H_2 loadings. This is consistent with a preferential-site-filling model and the general trend that the vibrational redshift scales with the site-specific adsorption enthalpy. As noted above, the primary Q and S bands of H_2 in MOF-74 display redshifts which are more than twice as large as those of MOF-5, an observation that is harmonious with the relative isosteric enthalpies of adsorption derived for these materials.[38] Using transmission IR spectroscopy, Vitillo *et al.* have observed an even larger vibrational redshift from H_2 in the isostructural Ni analog of MOF-74, and estimated its site-specific adsorption enthalpy to be ≈ -13.5 kJ/mol using a variable-temperature method.[30] Our preliminary data on the Co analog are also consistent with this trend, according to the isosteric analyses recently published for the known congeners of this series.[58] We are presently working on a complete investigation of the other analogs.

IV. SUMMARY

Diffuse reflectance IR spectra of H_2 adsorbed within the microporous material MOF-74 confirm the presence of discrete primary and secondary H_2 adsorption sites. Data reveal highly redshifted vibrational transitions with additional constrained translational and rotational quantum dynamics. The behavior of HD and D_2 diverge from the predictions of a

simple isotope effect, emphasizing the importance of the zero-point energy contribution. Concentration-dependent frequency shifts and *ortho* to *para* conversion rates provide further proof that the interactions among molecules adsorbed on neighboring sites are non-negligible. These realizations must be borne in mind while developing detailed theoretical models for H_2 physisorption in these materials.

ACKNOWLEDGMENTS

We thank Channing Ahn and Craig Brown for supplying us with a reference powder of MOF-74, and acknowledge the donors of the American Chemical Society Petroleum Research Fund and Research Corporation for their partial support of this research.

[1] P. Bénard and R. Chahine, Langmuir **17**, 1950 (2001).
[2] M. Latroche, S. Surblé, C. Serre, C. Mellot-Draznieks, P. L. Llewellyn, J.-H. Lee, J.-S. Chang, S. H. Jhung, and G. Férey, Angew. Chem., Int. Ed. **45**, 8227 (2006).
[3] M. Dincă, A. Dailly, Y. Liu, C. M. Brown, D. A. Neumann, and J. R. Long, J. Am. Chem. Soc. **128**, 16876 (2006).
[4] H. Furukawa, M. A. Miller, and O. M. Yaghi, J. Mater. Chem. **17**, 3197 (2007).
[5] S. Ma, J. Eckert, P. M. Forster, J. W. Yoon, Y. K. Hwang, J.-S. Chang, C. D. Collier, J. B. Parise, and H.-C. Zhou, J. Am. Chem. Soc. **130**, 15896 (2008).
[6] X. Lin, I. Telepeni, A. J. Blake, A. Dailly, C. M. Brown, J. M. Simmons, M. Zoppi, G. S. Walker, K. M. Thomas, T. J. Mays, P. Hubberstey, N. R. Champness, and M. Schröder, J. Am. Chem. Soc. **131**, 2159 (2009).
[7] H. Furukawa and O. M. Yaghi, J. Am. Chem. Soc. **131**, 8875 (2009).
[8] S. K. Bhatia and A. L. Myers, Langmuir **22**, 1688 (2006).
[9] P. M. Forster, J. Eckert, B. D. Heiken, J. B. Parise, J. W. Yoon, S. H. Jhung, J.-S. Chang, and A. K. Cheetham, J. Am. Chem. Soc. **128**, 16846 (2006).
[10] B. Panella, K. Hönes, U. Müller, N. Trukhan, M. Schubert, H. Pütter, and M. Hirscher, Angew. Chem., Int. Ed. **47**, 2138 (2008).
[11] S. R. Miller, G. M. Pearce, P. A. Wright, F. Bonino, S. Chavan, S. Bordiga, I. Margiolaki, N. Guillou, G. Férey, S. Bourrelly, and P. L. Llewellyn, J. Am. Chem. Soc. **130**, 15967 (2008).
[12] T. Yildirim and M. R. Hartman, Phys. Rev. Lett. **95**, 215504 (2005).
[13] E. C. Spencer, J. A. K. Howard, G. J. McIntyre, J. L. C. Rowsell, and O. M. Yaghi, Chem. Commun. (Cambridge) 2006, 278.
[14] V. K. Peterson, Y. Liu, C. M. Brown, and C. J. Kepert, J. Am. Chem. Soc. **128**, 15578 (2006).
[15] M. Dincă, W. S. Han, Y. Liu, A. Dailly, C. M. Brown, and J. R. Long, Angew. Chem., Int. Ed. **46**, 1419 (2007).
[16] H. Wu, W. Zhou, and T. Yildirim, J. Am. Chem. Soc. **129**, 5314 (2007).
[17] J. Luo, H. Xu, Y. Liu, Y. Zhao, L. L. Daemen, C. Brown, T. V. Timofeeva, S. Ma, and H.-C. Zhou, J. Am. Chem. Soc. **130**, 9626 (2008).
[18] B. L. Mojet, J. Eckert, R. A. van Santen, A. Albinati, and R. E. Lechner, J. Am. Chem. Soc. **123**, 8147 (2001).
[19] J. L. C. Rowsell, J. Eckert, and O. M. Yaghi, J. Am. Chem. Soc. **127**, 14904 (2005).
[20] F. M. Mulder, T. J. Dingemans, H. G. Schimmel, A. J. Ramirez-Cuesta, and G. J. Kearley, Chem. Phys. **351**, 72 (2008).
[21] C. M. Brown, Y. Liu, T. Yildirim, V. K. Peterson, and C. J. Kepert, Nanotechnology **20**, 204025 (2009).
[22] L. M. Kustov and V. B. Kazansky, J. Chem. Soc., Faraday Trans. **87**, 2675 (1991).
[23] A. Y. Khodakov, L. M. Kustov, V. B. Kazansky, and C. Williams, J. Chem. Soc., Faraday Trans. **88**, 3251 (1992).
[24] V. B. Kazansky, F. C. Jentoft, and H. G. Karge, J. Chem. Soc., Faraday Trans. **94**, 1347 (1998).
[25] S. Bordiga, J. G. Vitillo, G. Ricchiardi, L. Regli, D. Cocina, A. Zecchina, B. Arstad, M. Bjørgen, J. Hafizovic, and K. P. Lillerud, J. Phys. Chem. B **109**, 18237 (2005).
[26] C. Otero Areán, D. Nachtigallová, P. Nachtigall, E. Garrone, and M. Rodríguez Delgado, Phys. Chem. Chem. Phys. **9**, 1421 (2007).
[27] S. Bordiga, L. Regli, F. Bonino, E. Groppo, C. Lamberti, B. Xiao, P. S. Wheatley, R. E. Morris, and A. Zecchina, Phys. Chem. Chem. Phys. **9**, 2676 (2007).
[28] G. Spoto, J. G. Vitillo, D. Cocina, A. Damin, F. Bonino, and A. Zecchina, Phys. Chem. Chem. Phys. **9**, 4992 (2007).
[29] S. A. FitzGerald, K. Allen, P. Landerman, J. Hopkins, J. Matters, R. Myers, and J. L. C. Rowsell, Phys. Rev. B **77**, 224301 (2008).
[30] J. G. Vitillo, L. Regli, S. Chavan, G. Ricchiardi, G. Spoto, P. D. C. Dietzel, S. Bordiga, and A. Zecchina, J. Am. Chem. Soc. **130**, 8386 (2008).
[31] E. Garrone and C. Otero Areán, Chem. Soc. Rev. **34**, 846 (2005).
[32] A. Centrone, L. Brambilla, and G. Zerbi, Phys. Rev. B **71**, 245406 (2005).
[33] A. Centrone, D. Y. Siberio-Pérez, A. R. Millward, O. M. Yaghi, A. J. Matzger, and G. Zerbi, Chem. Phys. Lett. **411**, 516 (2005).
[34] B. Panella and M. Hirscher, Phys. Chem. Chem. Phys. **10**, 2910 (2008).
[35] J. L. C. Rowsell, E. C. Spencer, J. Eckert, J. A. K. Howard, and O. M. Yaghi, Science **309**, 1350 (2005).
[36] N. L. Rosi, J. Kim, M. Eddaoudi, B. Chen, M. O'Keeffe, and O. M. Yaghi, J. Am. Chem. Soc. **127**, 1504 (2005).
[37] P. D. C. Dietzel, R. E. Johnsen, R. Blom, and H. Fjellvåg, Chem.-Eur. J. **14**, 2389 (2008).
[38] J. L. C. Rowsell and O. M. Yaghi, J. Am. Chem. Soc. **128**, 1304 (2006).
[39] Y. Liu, H. Kabbour, C. M. Brown, D. A. Neumann, and C. C. Ahn, Langmuir **24**, 4772 (2008).
[40] G. Herzberg, *Molecular Spectra and Molecular Structure*, Spectra of Diatomic Molecules Vol. I (Kriegler, Malabar, Florida, 1989), reprinted.
[41] See supplementary material at http://link.aps.org/supplemental/10.1103/PhysRevB.81.104305 for detailed experimental description and results of thermogravimetric analyses and powder x-ray diffraction.

[42] As an aside, we note that the changes in the PXRD patterns reported by Rowsell *et al.* (Ref. 38) for their sample can be ascribed to partial rehydration during data acquisition, forming phase 2 described in Ref. 37. Outgassed MOF-74 is extremely hygroscopic and must be handled under a dry atmosphere at all times.

[43] S. A. FitzGerald, H. O. H. Churchill, P. M. Korngut, C. B. Simmons, and Y. E. Strangas, Rev. Sci. Instrum. **77**, 093110 (2006).

[44] L. Andrews and X. Wang, Rev. Sci. Instrum. **75**, 3039 (2004).

[45] A fourth site was also identified, forming a second layer within the channels at ≥ 3 D_2 per Zn.

[46] I. F. Silvera, Rev. Mod. Phys. **52**, 393 (1980).

[47] H. P. Gush, W. F. J. Hare, E. J. Allin, and H. L. Welsh, Can. J. Phys. **38**, 176 (1960).

[48] S. A. FitzGerald, H. O. H. Churchill, P. M. Korngut, C. B. Simmons, and Y. E. Strangas, Phys. Rev. B **73**, 155409 (2006).

[49] L. Kong, G. Román-Pérez, J. M. Soler, and D. C. Langreth, Phys. Rev. Lett. **103**, 096103 (2009).

[50] J. Vitko and C. F. Coll, J. Chem. Phys. **69**, 2590 (1978).

[51] C. Schwartz and R. Le Roy, J. Mol. Spectrosc. **121**, 420 (1987).

[52] M. E. Alikhani, B. Silvi, and J. P. Perchard, J. Chem. Phys. **90**, 5221 (1989).

[53] H. E. Hallam, *Vibrational Spectroscopy of Trapped Species* (Wiley, New York, 1973).

[54] G. Karl, J. D. Poll, and L. Wolniewicz, Can. J. Phys. **53**, 1781 (1975).

[55] A. Farkas, *Orthohydrogen, Parahydrogen, and Heavy Hydrogen* (Cambridge University Press, Cambridge, England, 1935).

[56] R. M. Herman and J. C. Lewis, Phys. Rev. B **73**, 155408 (2006).

[57] S. Mamone, M. Ge, D. Hüvonen, U. Nagel, A. Danquigny, F. Cuda, M. C. Grossel, Y. Murata, K. Komatsu, M. H. Levitt, T. Rõõm, and M. Carravetta, J. Chem. Phys. **130**, 081103 (2009).

[58] W. Zhou, H. Wu, and T. Yildirim, J. Am. Chem. Soc. **130**, 15268 (2008).